An Evaluation Circuit for DC-Link Capacitors used in a Single-Phase PWM Inverter

Kazunori Hasegawa, Kyushu Institute of Technology, Japan, hasegawa@life.kyutech.ac.jp
Ichiro Omura, Kyushu Institute of Technology, Japan, omura@ele.kyutech.ac.jp
Shin-ichi Nishizawa, Kyushu University, Japan, s.nishizawa@riam.kyushu-u.ac.jp

Abstract

High-power conversion systems are based not only on three-phase inverters but also on single-phase inverters because modular multilevel cascade converters (MMCC) consist of half- or full-bridge single-phase converters. Their DC-link capacitors are a major constraint on the improvement of power density as well as of reliability. Evaluation of dc-link capacitors in terms of power loss, ageing, and failure rate will play an important role in the next-generation power converters. This paper presents an evaluation circuit for dc-link capacitors used in a high-power single-phase PWM inverter. The evaluation circuit produces a practical ripple current waveform and a dc bias voltage into a capacitor under test with a downscaled voltage-rating inverter, which is equivalent to those of the full-scale inverter. Theoretical analysis and experimental results verify the effectiveness of the evaluation circuit.

1. Introduction

DC-link capacitors in power electronic converters are a major constraint on the improvement of power density [1]. They tend to include a design margin of size or capacitance due to power loss. The minimum design margin of the capacitors is desirable. A lifetime of the capacitors is usually shorter than that of semiconductor devices or magnetic devices. Evaluation of the capacitors in terms of power loss, ageing, and failure rate will play an important role in design stages of the next-generation power converters [2-12]. However, characteristics of the capacitors are usually evaluated by a single sinusoidal current such as 120 Hz, 1 kHz, and so on [5-7]. There are some kinds of “ripple current tester” instruments that provide a sinusoidal ripple current as well as a dc-bias voltage into the capacitor [5]. Actual current flowing out of the converter into the capacitor contains multiple frequency components, so that characteristics of the capacitors cannot be exactly estimated [8]. In addition, the dc bias voltage across the capacitors affects power loss and ageing [3,7]. Thus, existing power converters often employ more capacitors than necessary. It is important to develop an evaluation circuit that will be utilized in design stages or in tests before shipment of the converters. Note that the circuit should behave as an existing inverter in terms of the dc bias voltage and ripple current waveform of the capacitor.

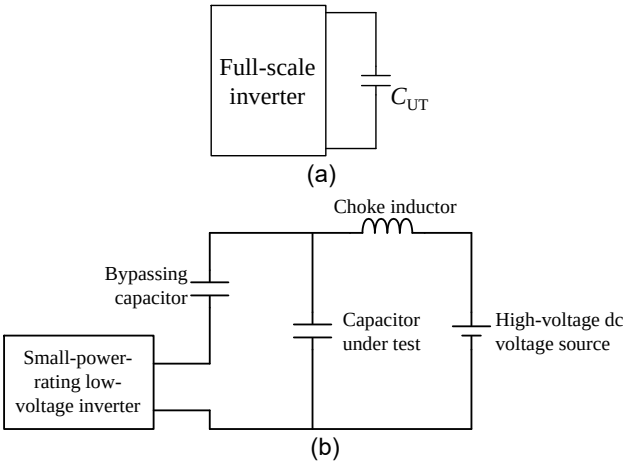

Fig. 1 Basic concepts of an evaluation circuit for a high-power capacitor. (a) Using full-scale inverter. (b) Using full-scale current-rating and downscale voltage-rating inverter.

The authors of this paper have proposed a new evaluation circuit using a small inverter for dc-link capacitors used in a high-power three-phase inverter [9, 10], which presents the equivalent current waveform to that of existing three-phase inverters. The evaluation circuit will be utilized for evaluating the capacitor such as the followings:

1) Electrical measurement of ESR and capacitance [4, 6, 11].
2) Power loss measurement [12, 13].
3) Accelerated aging [7].

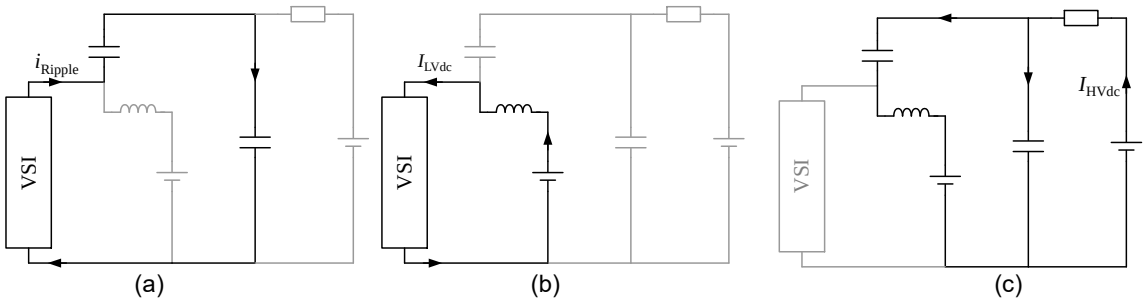

Fig. 3 Basic operation of the VSI-based evaluation circuit. (a) Ripple current flowing out of the VSI. (b) DC curren t flowing out of the low-voltage dc supply. (c) DC current flowing out of the high-voltage dc supply.

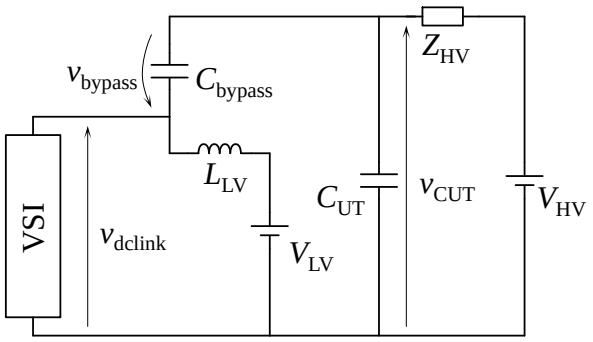

Fig. 2 VSI-based evaluation circuit

High-power conversion systems including AC motor drives and Flexible AC transmission systems (FACTS) are based not only on three-phase inverters but also on single-phase inverters because modular multilevel cascade converters (MMCC) [14-16], that are also referred to “modular multilevel converters (MMC)” or “cascaded H-bridge converters (CHB), consist of single-phase full-bridge or half-bridge converters. Therefore, an evaluation circuit for dc-link capacitors used in a high-power single-phase inverter is also attractive for practical use.

This paper describes the performance of the evaluation circuit when it is applied to a single-phase high-power PWM inverter. Theoretical analysis reveals the lower limit of the power rating. Experimental results confirm the effectiveness of the circuit.

2. Evaluation Circuit for DC-link Capacitors Based on Voltage-Source Inverters

2.1. Basic Concept

The most effective way to evaluate dc-link capacitors is measuring their characteristics with an existing converter in operation. Fig. 1 (a) shows the basic idea of the evaluation circuit, in which a full-scale current-rating and full-scale voltage-rating inverter is connected to a capacitor under test, C_{UT}.

Fig. 1 (b) shows the basic concept of the new evaluation circuit that employs a small-power-rating inverter, the capacitor under test, a bypassing capacitor, a choke inductor, and a high-voltage dc supply [9]. The concept is similar to the circuits proposed in [6] and [7] in terms of the combination of a ripple current generator and a dc voltage supply, whereas it presents the same current waveform as that generated by the inverter. The current rating of the small inverter is full-scale, while voltage rating of that is downscale. The high-voltage dc supply keeps the capacitor voltage a desired dc bias voltage. The bypassing capacitor is used for circulating the ripple current generated by the inverter through the capacitor under test. The choke inductor blocks the ripple current, through which only dc current flows. Hence, the new circuit operates as the full-scale voltage-rating and full-scale current-rating inverter from the standpoint of the dc bias voltage and ripple current. Note that the choke inductor L_{HV} can be replaced by a resistor if its dissipated power is negligible.

2.2. Voltage-Source-Converter-Based Circuit

Voltage-source inverters (VSIs) can be used as the small inverter [9, 10]. Fig. 2 shows the VSI-based evaluation circuit, where the VSI stands for either a three-phase full-bridge inverter or a single-phase one. The dc-link terminal of the VSI is connected to the bypassing capacitor and the capacitor under test. The three-phase-VSI-based circuit behaves as a full-scale three-phase inverter, whereas the single-phase-VSI-based circuit does a full-scale single-phase inverter as well.

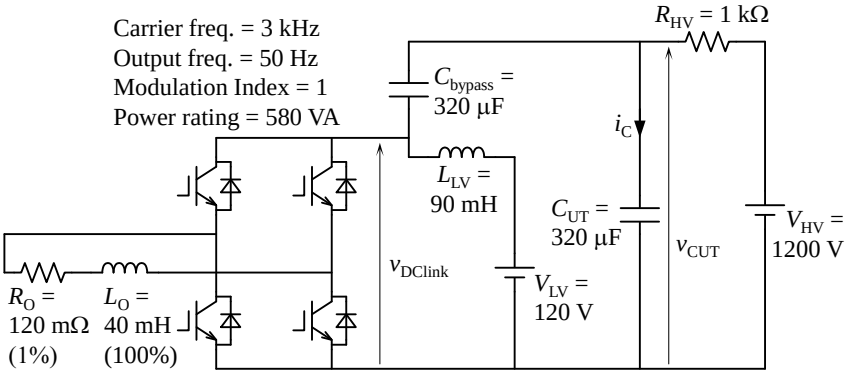

Fig. 4 Experimental setup of the evaluation circuit consisting of a single-phase inverter and its circuit parameters.

Fig. 3 shows current paths of the VSI-based circuit. The ripple current generated by the VSI circulates through C_{bypass} and C_{UT} as shown in Fig. 3(a). The low-voltage dc supply V_{LV} provides a dc current to the VSI through L_{LV}, as shown in Fig. 3(b). The high-voltage dc supply charges C_{UT} and C_{bypass} to its operating voltage, and then supplies a small amount of leakage dc current of the capacitors as shown in Fig. 3(c). Hence, the power rating of the high-voltage dc supply is quite small.

Note that the evaluation circuit using a single-phase current-source inverter (CSI) can also behave as the full-scale three-phase and single-phase inverter if it can provide the same ripple current waveform as that generated by the full-scale single-phase and three-phase inverter, respectively. However, not only pulse width but also amplitude should be modulated to synthesize the ripple current waveform. In practice, therefore, quite complex control would be required for the CSI [9, 10].

3. Application to a Single-Phase Inverter

3.1 Power Rating of the small VSI

Since the current rating of the low-voltage inverter is the same as that of the full-scale inverter, the relation between the power rating of the small VSI, P_{Small} and that of the full-scale inverter, P_{FS} is given by

$$n = \frac{P_{\mathrm{Small}}}{P_{\mathrm{FS}}} = \frac{V_{\mathrm{DClink-S}}}{V_{\mathrm{DClink-FS}}} = \frac{V_{\mathrm{LV}}}{V_{\mathrm{HV}}}, \tag{1}$$

where $V_{DClink-FS}$ and $V_{DClink-S}$ are nominal dc-link voltages of the full-scale inverter and the VSI, respectively. As for determining V_{LV}, attention should be paid to the ripple amplitude of the dc-link voltage because the ripple amplitude must be smaller than the nominal dc-link voltage always to keep the dc-link voltage positive.

3.1 Ripple Voltage on the DC Link

A major concern of the evaluation circuit consisting of the single-phase VSI is the ripple amplitude of the capacitor voltage under test because instantaneous power in a single-phase circuit fluctuates at double the fundamental frequency, whereas that in a three-phase circuit is constant [17].

The dc-link voltage of the VSI, v_{dclink}, is the sum of the v_{bypass} and v_{CUT}, as shown in Fig. 1(b), so that the ripple amplitude of the dc-link voltage, Δv_{dclink}, is given by

$$\Delta v_{dclink} = \Delta v_{bypass} + \Delta v_{CUT} \tag{1}$$

where Δv_{bypass} and Δv_{CUT} stand for ripple amplitudes of those of the two capacitors. Δv_{dclink} is a constraint on the power rating of the VSI because the dc mean of the dc-link voltage V_{dclink} should be designed to be larger than ripple amplitude. From equation (1), the ripple ratio of v_{dclink}, r_{dclink} is given by

$$\begin{aligned} r_{dclink} &= \frac{\Delta v_{dclink}}{V_{LV}} = \frac{\Delta v_{bypass} + \Delta v_{CUT}}{V_{LV}} \\ &= \frac{\Delta v_{bypass} + \Delta v_{CUT}}{V_{HV}} \times \frac{V_{HV}}{V_{LV}} \\ &= \left(r_{bypass} + r_{CUT}\right) \times \frac{1}{n} \end{aligned} \tag{2}$$

where r_{bypass} and r_{CUT} are ripple ratios of v_{bypass} and v_{CUT} with respect to V_{HV}, respectively. n corresponds to the ratio between voltage ratings of the full-scale inverter and the small inverter. Equation (2) suggests that the dc-link voltage

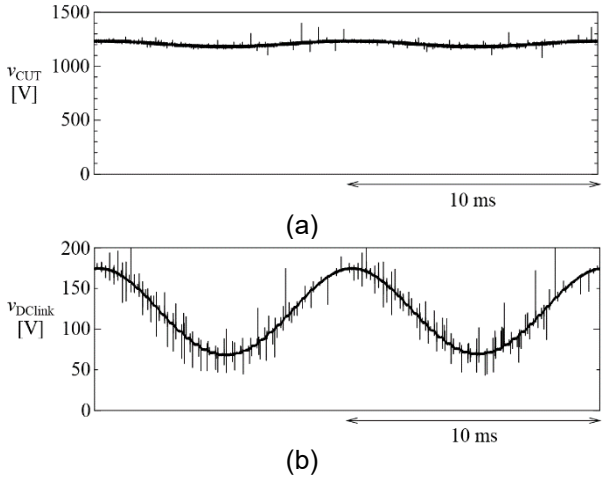

Fig. 5 Voltage waveforms of the single-phase-VSI-based circuit. (a) v_{CUT}. (b) v_{dclink}.

could contain a large ripple amplitude although the two capacitors contain a small ripple ratio. r_{dclink} has to be less than unity in order not to make the dc-link voltage negative as follows:

$$r_{dclink} < 1 \tag{3}$$

Substituting (2) into (3) gives

$$r_{bypass} + r_{CUT} < n \tag{4}$$

Equation (4) suggests that ripple ratios of C_{bypass} and C_{UT} determine the lower limit of the power rating of the small VSI. For example, if both the ripple ratios r_{bypass} and r_{CUT} is 5%, the power rating of the VSI should be more than 1/10 of that of the full-scale inverter.

3.3 Design of Choke Inductors

The ripple current contains the switching frequency and double the output frequency (2ω) components of the VSI. The low-voltage choke inductor L_{LV} and choke impedance Z_{HV} should block both the switching frequency and 2ω components. Since 2ω is much lower than the switching frequency, only 2ω can be taken into account for the design of the low-voltage choke inductor L_{LV} and choke impedance Z_{HV}.

Impedances of L_{LV} and Z_{HV} should be much larger than that of capacitors C_{UT} and C_{bypass}.

$$2\omega L_{LV} \gg \frac{1}{2\omega C_{dc}} \tag{5}$$

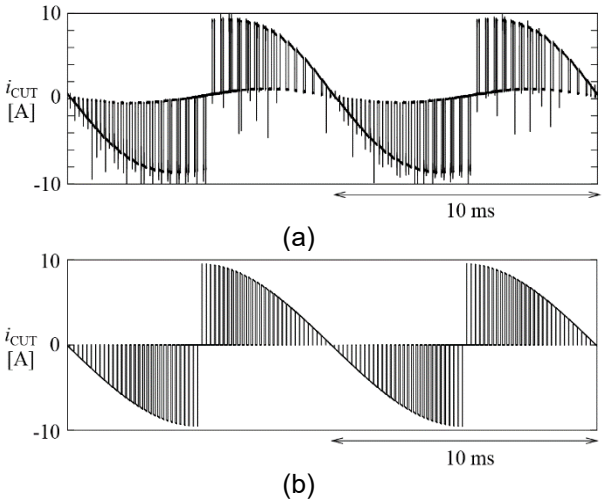

Fig. 6 Current waveforms of the single-phase-VSI-based circuit. (a) Experimental waveform of the evaluation circui t. (b) Simulated waveform of the Full-scale inverter.

$$Z_{HV}(2\omega) \gg \frac{1}{2\omega C_{dc}} \tag{6}$$

where $\omega = 2\pi f_O$, f_O is the output frequency of the inverter, C_{dc} indicates C_{UT} or C_{bypass}. This paper introduced a L_{LV} of 90 mH that is 56 Ω at 100 Hz, while either C_{bypass} or C_{UT} had an impedance of 5 Ω at 100 Hz for experiment.

4. Experiment

4.1 Experimental Circuit Configuration

Fig. 4 shows the experimental setup of the evaluation circuit and its circuit parameters. The circuit employs 320-μF metalized polypropylene capacitors rated at 1200 V for C_{UT} and C_{bypass}. The unit capacitance constant of the capacitor is 40 ms [18]. The low-voltage dc supply V_{LV} is adjusted to be 1/10 of V_{HV}. Although the power rating of the VSI is 580 VA, the evaluation circuit act as a 5800-VA inverter for the capacitor under test. Sinusoidal pulse-width modulation is applied to the inverter with a unity modulation index.

4.2 Results

Figs. 5 shows voltage waveforms of v_{CUT} and v_{dclink}, where v_{CUT} fluctuated at double the output frequency, 100 Hz. The ripple ratio of the capacitor under test r_{CUT} was 5% (60 V), while that of the dc-

link voltage r_{dclink} was 88% (105 V) that is almost 10 times as large as the sum of r_{CUT} and r_{bypass}, which agreed with equation (2). Fig. 6 shows current waveforms flowing into the capacitor under test, i_{CUT}, and also show that in a 5800-VA full-scale three-phase inverter by simulation for comparison, where a software package of "PLECS" is carried out [19]. The waveform of the evaluation circuit almost agreed with that of the full-scale inverter although the dc-link voltage contained a large amount of ripple component.

Conclusion

This paper presents the performance of an evaluation circuit for dc-link capacitors, consisting of a single-phase voltage-source PWM inverter. Although the power rating of the evaluation circuit suffers from a ripple voltage resulting from double the fundamental frequency component unlike a three-phase inverter, it can be 1/10 of the full-scale inverter in practice. Experimental results have confirmed that the circuit produced almost the same current ripple current waveform into a capacitor under test as that of the full-scale inverter.

The evaluation circuit will provide accurate power-loss measurement and lifetime estimation for dc-link capacitors used in high-power single-phase-inverter-based circuit like modular multilevel converters.

Acknowledgement

The authors would like to thank Prof. Keiji Wada of Tokyo Metropolitan University, Tokyo, Japan, for his fruitful discussions.

References

[1] J. W. Kolar, U. Drofenik, J. Biela, M. Heldwein, H. Ertl, T. Friedli, and S. Round, "PWM converter power density barriers," *IEE Japan Trans. Ind. Appl.*, vol. 128, no. 4, pp.468-480, 2008

[2] H. Wang and F. Blaabjerg, "Reliability of capacitors for dc-ink applications in power electronic converters—an overview," *IEEE Trans. Ind. Appl*. vol. 50, no. 5, pp. 3569-3578, 2014.

[3] P. Venet, F. Perisse, M. H. El-Husseini, and G. Rojat, "Realization of a smart electrolytic capacitor circuit," *IEEE Ind. Appl. Mag*., vol. 8, no. 1,pp. 16–20, Jan./Feb. 2002.

[4] E. C. Aeloiza, J. H. Kim, P. Ruminot, and P. N. Enjeti, "A Real Time Method to Estimate Electrolytic Capacitor Condition in PWM Adjustable Speed Drives and Uninterruptible Power Supplies," IEEE Power Electronics Specialists Conference (PESC), pp. 2867-2872, 2005.

[5] *RIPPLE CURRENT TESTER MODEL 11800/11801/11810*, Chroma ATE Inc. 2014. [Online]. available: http://www.chromaate.com/File/DownLoad/42014

[6] A. M. R. Amaral, and A. J. M. Cardoso, "Estimating aluminum electrolytic capacitors condition using a low frequency transformer together with a dc power supply," *in Proc. of IEEE ISIE*, pp. 815-820, 2010.

[7] M. Makdessi, A. Sari, P. Venet, P. Bevilacqua, and C. Joubert, "Accelerated Ageing of Metallized Film Capacitors Under High Ripple Currents Combined With a DC Voltage," *IEEE Trans. Power Electron*., vol. 30, no. 5, pp. 2435-2444, May 2015.

[8] K. Hasegawa, K. Kozuma, K. Tsuzaki, I. Omura, and S. Nishizawa, "Temperature rise measurement for power-loss comparison of an aluminium electrolytic capacitor between sinusoidal and square-wave current injections," *Microelectron. Rel*., vol. 64, pp. 98-100, 2016.

[9] K. Hasegawa, I. Omura, and S. Nishizawa, "Design and Analysis of a New Evaluation Circuit for Capacitors Used in a High-Power Three-Phase Inverter," *IEEE Trans. Ind. Electron*., vol. 63, no. 5, pp. 2679-2687, May 2015.

[10] K. Hasegawa, I. Omura, and S. Nishizawa, "A New Evaluation Circuit with a Low-Voltage Inverter Intended for Capacitors Used in a High-Power Three-Phase Inverter," *IEEE APEC*., pp. 3032-3037, Mar. 2016.

[11] K. Abdennadher, P. Venet, G. Rojat, J. M. Retif, and C. Rosset, "A Real-Time Predictive-Maintenance System of Aluminum Electrolytic Capacitors Used in Uninterrupted Power Supplies," *IEEE Trans. Ind. Appl.* vol. 46, no. 4, pp. 1644-1652, Jul./Aug., 2010.

[12] J. M. Miller, C. W. Ayers, L. E. Seiber, and D. B. Smith, "Calorimeter evaluation of inverter grade metalized film capacitor ESR," in Proc. of IEEE ECCE, pp. 2157-2163, 2012.

[13] D. Christen, U. Badstuebner, J. Biela, and J.W. Kolar, "Calorimetric power loss measurement for highly efficient converters," in Conf. Rec. of International Power Electronics Conference (IPEC), pp. 1438-1445, 2010.

[14] P. W. Hammond, "A new approach to enhance power quality for medium voltage ac drives", *IEEE Trans. Ind. Appl.*, vol. 33, no. 1, pp. 202-208, 1997.

[15] H. Akagi, "Classification, Terminology, and Application of the Modular Multilevel Cascade Converter (MMCC)," *IEEE Trans. Power Electron*., vol. 26, no. 11, pp. 3119-3130, 2011.

[16] T. Nakanishi, J. Itoh: "Control Strategy for Modular Multilevel Converter based on Single-phase Power Factor Correction Converter ", IEEJ J. Ind. Appl., Vol. 6, No. 1, pp. 46-57, 2017.

[17] H. Akagi, Y. Kanazawa, and A. Nabae, "Instantaneous reactive power compensators comprising switching devices without energy storage components," IEEE Trans. Ind. Appl., vol. IA-20, no. 3, pp. 625-630, 1984.

[18] H. Fujita, S. Tominaga, and H. Akagi, "Analysis and design of a dc voltage-controlled static var compensator using quad-series voltage-source inverters," IEEE Trans. Ind. Appl., vol. 32, no. 4, pp. 970--977, 1996.

[19] [Online]. available: http://www.plexim.com/plecs